https://doi.org/10.5194/acp-2022-544
Preprint. Discussion started: 22 August 2022

Atmospheric Chemistry and Physics Discussions

Size dependent hygroscopicity of levoglucosan and D-glucose aerosol nanoparticles

Ting Lei[1,2], Hang Su[2,3], Nan Ma[4], Ulrich Pöschl[2], Alfred Wiedensohler[5], Yafang Cheng[1]

[1]Minerva Research Group, Max Planck Institute for Chemistry, 55128 Mainz, Germany

[2]Multiphase Chemistry Department, Max Planck Institute for Chemistry, 55128 Mainz, Germany

[3]State Environmental Protection Key Laboratory of Formation and Prevention of Urban Air Pollution Complex, Shanghai Academy of Environmental Sciences, Shanghai 200233, China

[4]Institute for Environmental and Climate Research, Jinan University, 511443 Guangzhou, China

[5]Leibniz Institute for Tropospheric Research, 04318 Leipzig, Germany

Correspondence to: Yafang Cheng (yafang.cheng@mpic.de)

Abstract: The interaction between water vapor and aerosol nanoparticles is of great significance in atmospheric processes. However, current knowledge of hygroscopicity of sub-10 nm organic nanoparticles and their concentration-dependent thermodynamic properties (e.g., water activity) in the highly supersaturated concentration range is scarcely available. In this study, we investigate the size dependence of hygroscopicity of organics (i.e., levoglucosan, D-glucose) in size down to 6 nm using a nano-hygroscopicity tandem differential mobility analyzer (nano-HTDMA). There is a weak size dependence of the hygroscopic growth factor observed for levoglucosan and D-glucose nanoparticles with diameters down to 20 nm. However, a clear size-dependent hygroscopic growth factor is observed for D-glucose nanoparticles down to 6 nm in size. A reduction in diameters of sub-20 nm levoglucosan is observed at the dry RHs, which is explained by partial levoglucosan evaporation into gas phase, indicting high impact of volatility of sub-20 nm levoglucosan aerosol

https://doi.org/10.5194/acp-2022-544
Preprint. Discussion started: 22 August 2022


Atmospheric Chemistry and Physics Discussions

nanoparticles. However, this also means that the hygroscopic growth factors of levoglucosan nanoparticles with diameters below 20 nm are not possible to be determined. The use of water activity parameterization models proposed by Kreidenweis et al. (2005) (KD, Köhler), the Extend-Aerosol Inorganic Model (E-AIM (standard UNIFAC), and Differential Köhler Analysis (DKA) method is to determine thermodynamic properties (e.g., water activity) of levoglucosan and D-glucose nanodroplets as a function of solute concentration, respectively. Predicated water activity for these aqueous organic solutions (i.e., levoglucosan, D-glucose) from the different methods are similar to observations from references in the low solute concentration (< 20 mol kg^{-1}), while a quite difference is found in the high solute concentration (> 20 mol kg^{-1}). In addition, we compare hygroscopicity measurements for levoglucosan and D-glucose nanoparticles with the E-AIM (standard UNIFAC), the ideal solution theory, and DKA predictions, respectively. The ideal solution theory describes well the measured hygroscopic growth factors of levoglucosan with diameters down to 20 nm and D-glucose nanoparticles with diameters higher than 60 nm, respectively, while the E-AIM (standard UNIFAC) model can successfully predict the growth factors of levoglucosan with diameters from 100 down to 6 nm at RH above 88-40 % (e.g., at RH above 88 % for 100 nm D-glucose, at RH above 40 % for 6 nm D-glucose). The use of the DKA method leads to a good agreement with measured hygroscopic growth factors of D-glucose aerosol nanoparticles with diameters from 100 down to 6 nm.

1 Introduction

Organic aerosol nanoparticles play an important role in new particle formation, subsequent condensation and coagulation growth, cloud condensation nuclei (CCN), and thus in affecting visibility degradation, radiative forcing, and climate (Chylek and Coakley, 1974; Charlson et al.,

https://doi.org/10.5194/acp-2022-544
Preprint. Discussion started: 22 August 2022

Atmospheric Chemistry and Physics Discussions

1992; Dusek et al., 2010; Cheng et al., 2012; Zhang et al., 2012; Kulmala et al., 2013). Both growth of nanoparticles and their ability to act as CCN are directly related to its hygroscopicity that describes the interaction between organic nanoparticles and water vapor (Köhler, 1936; Kreidenweis et al., 2005; Su et al., 2010; Cheng et al., 2015; Wang et al., 2015). However, current knowledge of hygroscopicity of sub-10 nm organic nanoparticles and their concentration-dependent thermodynamic properties (e.g., water activity) in the highly supersaturated concentration range is scarcely available.

Levoglucosan aerosol nanoparticles have attracted increasing interest in recent years (Simoneit et al., 1999; Mochida and Kawamura, 2004; Mikhailov et al., 2009; Elias et al., 2010; Lei et al., 2014, 2018; Bhattarai et al., 2019) due to relative stability and high emission factors, which are considered as an ideal tracer for characterization and quantitation the biomass burning (Fraser and Lakshmanan, 2000). Also, levoglucosan is typically the most abundant species in wood burning aerosols, which contributes substantially (16.6–30.9% by mass) to the total organics in $PM_{2.5}$ (Mochida and Kawamura, 2004). D-glucose, a hydrolysis product of cellulose and levoglucosan, is a major pyrolysis product of wood (Mochida and Kawamura, 2004). Levoglucosan and D-glucose substances may be representative in reproducing the hygroscopic behavior of the real biomass burning aerosol particles (Bhandari and Bareyre. 2003; Mochida and Kawamura, 2004; Chan et al., 2005; Koehler et al., 2006; Peng et al., 2010). Most of the previous lab studies have been focused on investigation of the hygroscopic behavior of 100-nm levoglucosan and D-glucose aerosol nanoparticles, which mainly utilized the humidified tandem differential mobility analyzers (DMAs) (Mikhailov et al., 2004; Mochida and Kawamura. 2004; Koehler et al., 2006; Lei et al., 2014; 2018). For example, Mochida and Kawamura (2004) observed that 100-nm levoglucosan and D-glucose aerosol nanoparticles uptake/release water continuously in both deliquescence and

https://doi.org/10.5194/acp-2022-544
Preprint. Discussion started: 22 August 2022


Atmospheric Chemistry and Physics Discussions

efflorescence modes, respectively. To our knowledge, there are no phase transitions for these organic aerosol nanoparticles in both hydration and dehydration processes.

Early studies showed that the hygroscopicity and solubility of inorganic aerosols, such as ammonium sulfate (AS) and sodium chloride (NaCl), exhibited a strong size dependence (Cheng et al., 2015). Firstly, hygroscopic diameter growth factors of AS, NaCl as well as Na_2SO_4 nanoparticles are found to decrease with size decreases in both deliquescence and efflorescence modes (Biskos et al., 2006a, b, c, Lei et al., 2020). Secondly, there is no significant difference in the deliquescence relative humidity (DRH) and the efflorescence relative humidity (ERH) between AS nanoparticles with dry diameters of 6 and 60 nm (Biskos et al., 2006b; Lei et al., 2020), while a pronounced size dependence of the DRH of NaCl is up to 10 % RH between dry diameters of 6 and 60 nm (Biskos et al., 2006a). The behaviors of change of phase transition RH and concentrations of Na_2SO_4 are between NaCl and AS (Lei et al., 2020). However, there are very few lab studies on investigating hygroscopicity (g_f, DRH, ERH) of organic aerosol nanoparticles in sub-10 nm size range (Wang et al., 2017). It is not clear how the size effect is going to influence the hygroscopic growth of organics, especially with no DRH and ERH. Besides technique limitation (Lei et al., 2020; Wang et al., 2017), another reason is the high diffusion of sub-100 nm organics nanoparticles, especially in the sub-10 nm size range, which results in nanoparticle losses in the HTDMA system (Seinfeld and Pandis, 2006).

For inorganic aerosols, the lack of thermodynamic properties of the highly supersaturated aqueous solution nanodroplets (Tang and Munkelwitz, 1994; Tang 1996; Pruppacher and Klett, 1997; Clegg et al., 1998) are limiting predictability of aerosol hygroscopic behavior of sub-10 nm aerosol nanoparticles (Cheng et al., 2015). Also, there are very few thermodynamic data in the highly supersaturated concentration for organic solution, such as levoglucosan and D-glucose (Bhandari

https://doi.org/10.5194/acp-2022-544
Preprint. Discussion started: 22 August 2022


Atmospheric Chemistry and Physics Discussions

and Bareyre. 2003; Chan et al., 2005; Koehler et al., 2006; Peng et al., 2010). By measuring the hygroscopic growth factor of particles of different sizes, we may be able to retrieve these thermodynamic data using a Differential Köhler Analysis (DKA) method (Cheng et al., 2015). This will further help us to understand the new particle formation, transportation, and their interactions between water molecules.

In this study, we investigate the hygroscopic growth factors of levoglucosan and D-glucose nanoparticles in size down to 6 nm using a nano-hygroscopic tandem differential mobility analyzer (nano-HTDMA, Lei et al., 2020). Moreover, we compare our measurement data with model prediction from the Extended Aerosol Inorganic Model (E-AIM (standard UNIFAC)) (Clegg et al., 2001; Clegg and Seinfeld, 2006; available online: http://www.aim.env.ac.uk/aim/aim.php), the ideal solution theory, and DKA. In addition, the use of the DKA method is to calculate thermodynamic properties (e.g., water activity) of D-glucose nanodroplets in the highly supersaturated concentration range and then to compare with KD-derived data (KD=Kreidenweis), thermodynamic property data from Köhler (Kreidenweis et al., 2005), E-AIM (standard UNIFAC) model, and references, respectively.

2 Methodology

2.1 Experimental methods

2.1.1 Nanoparticle generation

An electrospray is employed to generate levoglucosan and D-glucose aerosol nanoparticles of 6, 8, 10, and 15 nm using 2, 3, 5, and 10 mM aqueous solutions with 50 % volume fraction of a 20 mM ammonium acetate buffer solution (Chen et al., 2005; Wang et al., 2015), respectively. The

https://doi.org/10.5194/acp-2022-544
Preprint. Discussion started: 22 August 2022

Atmospheric Chemistry and Physics Discussions

generated nanoparticles are diluted by mixing with dry and filtered N_2 (1 l/min) and CO_2 (0.1 l/min), bringing aerosol nanoparticles to a dry RH state (≤ 2% RH). Subsequently, aerosol nanoparticles pass through a Po^{210} neutralizer to reach the equilibrium charge distribution (Wiedensohler 1986). In order to avoid blocking the 25-μm capillary tube in the electrospray with high solution concentration, the aerosol nanoparticles with diameters of 60-100 and 20 nm are generated by an atomizer with a 0.05 and 0.01 wt % organic solution (i.e., levoglucosan and D-glucose), respectively. The chemical substances and their physical properties are characterized in Table S1. These solutions are prepared with distilled and de-ionized million-Q water (resistivity of 18.2 MΩ cm at 298.15 K). Note that, the size selected by the nano-DMA1 should be the right part of peak diameter of the number size distribution of the generated nanoparticles, which minimizes the influence of the multiple charged nanoparticles in hygroscopicity measurements.

2.1.2 Nano-HTDMA setup

Figure 1 shows a schematic of the nano-HTDMA system for investigating the hygroscopic behavior of aerosol nanoparticles, especially in the sub-10 nm size range. The detailed description, calibration, and validation of nano-HTDMA setup have been reported in the previous paper (Lei et al., 2020). In brief, the polydisperse aerosol nanoparticles pass through a silica gel diffusion dryer and a Nafion gas dryer (TROPOS Model ND.070, Length 60 cm). The dry aerosol nanoparticles at RH below 10 % are charged by a Kr^{85} bipolar charger and then enter the first nano-differential mobility analyzer (nano-DMA1, TROPOS Model Vienna-type short DMA), where a monodisperse distribution of nanoparticles with the desired dry diameter is selected. The monodispersed nanoparticles subsequently are exposed to the different RH conditions, which can be set to deliquescence mode (from low RH to high RH for measuring deliquescence) or efflorescence mode (from the high RH to low RH for measuring efflorescence). In the deliquescence mode, the dry

https://doi.org/10.5194/acp-2022-544
Preprint. Discussion started: 22 August 2022

Atmospheric Chemistry and Physics Discussions

aerosol nanoparticles are gradually humidified to a target RH through a Nafion humidifier (NH-1, TROPOS Model ND.070, Length 60 cm). In the efflorescence mode, after deliquescence of aerosol nanoparticles with RH above 97% in a Nafion humidifier (NH-2: Perma Pure Model MH-110, Length 30 cm), the deliquesced aerosol nanoparticles are stepwise dried to a target RH in NH-1. The number size distribution of the humidified nanoparticles is then measured by a nano-differential mobility analyzer (nano-DMA2) at a target RH through a Nafion humidifier (NH-3, Perma Pure Model PD-100) coupled with an ultrafine condensation particle counter (CPC, TSI, model no. 3776). To have the uniform RH within the nano-DMA2 for the accurate determination of hygroscopicity (g_f, DRH, ERH) of aerosol nanoparticles, the difference between the sheath flow RH (RH_s) and the aerosol flow RH (RH_a) upstream of the nano-DMA2 is kept <1 %. Most importantly, the temperature difference between inlet and outlet of the nano-DMA2 is maintained below 0.2 °C during the measurements. In addition, the residence time (e.g., 5.4 s: between the humidifier and the nano-DMA2; 0.07 s: deliquescence for aerosol nanoparticles) is sufficient for water-soluble aerosol nanoparticles to equilibrate with water vapor at a given RH and to occur solid-liquid phase transition (Kerminen 1997; Duplissy et al., 2005; Raoux et al., 2007), respectively.

2.2 Theory and modeling methods

2.2.1 Köhler theory

The fractional ambient relative humidity ($\frac{RH}{100}$) over a spherical droplet in equilibrium with the environment is described by Köhler equation (Köhler 1936):

$$\frac{RH}{100} = a_w exp\left(\frac{4\sigma_{sol}v_w}{RTG_f D_s}\right) \quad (1)$$

https://doi.org/10.5194/acp-2022-544
Preprint. Discussion started: 22 August 2022


Atmospheric Chemistry and Physics Discussions

where a_w is the water activity of the solution droplet, σ_{sol} is the liquid-vapor interfacial energy of solution droplet (also called surface tension), v_w is the partial molar volume of water, R is the universal gas constant, T is the temperature, G_f is the diameter growth factor of aerosol particles, and D_s is the dry diameter of spherical aerosol particles. The hygroscopic growth curve (G_f vs RH) is estimated based on the assumptions in models or theories described in the following sections (2.2.2-2.2.3).

2.2.2 Water activity

2.2.2.1 Köhler

The expression for water activity used in the simplified Köhler theory assumes the droplet contains n_w moles of water and n_s moles of nonvolatile solute.

$$a_w = \frac{n_w}{n_w + \nu n_s} \quad (2)$$

ν is the number of ions of solute present in solution (ν=1 for organic composition). This expression has been applied to the diluted solution (Kreidenweis et al., 2005; Koehler et al., 2006).

2.2.2.2 KD

The following KD expression is proposed by Kreidenweis et al. (2005) (KD= Kreidenweis) is to present the relationship between a_w and *Gf* determined in hygroscopic growth measurements:

$$Gf = \left[1 + (a + b * a_w + c * a_w^2)\frac{a_w}{1-a_w}\right]^{\frac{1}{3}} \quad (3)$$

The coefficients a, b, and c for organic solution droplet in this study from Lei et al. (2014, 2018) and Estillore et al. (2017) as shown in Table S2.

2.2.2.3 DKA

https://doi.org/10.5194/acp-2022-544
Preprint. Discussion started: 22 August 2022


Atmospheric Chemistry and Physics Discussions

Differential Köhler analysis (DKA) proposed by Cheng et al. (2015) is theoretically based on Köhler equation (Köhler, 1936) to determine water activity by measuring hygroscopic growth factors of aerosol nanoparticles in different sizes.

$$a_w = \frac{s_{w1}^{\left(\frac{D_{s1}}{D_{s1}-D_{s2}}\right)}}{s_{w2}^{\left(\frac{D_{s2}}{D_{s1}-D_{s2}}\right)}} \quad (4)$$

where $A = \frac{4v_w}{RTg_f}$, s_{w1} and s_{w2} are water saturation ratio measured at the same g_f but at the different initial dry diameters (D_{s1}, D_{s2}), respectively. Using the DKA method can calculate the water activity in the highly supersaturated concentration range.

2.2.3 Growth factor

2.2.3.1 Ideal solution growth factor

For idea solution, the hygroscopic curve can be estimated assuming that the water activity a_w of the solution containing non-volatile and non-electrolyte solute component is equal to the molar ratio of water in the solution. Here, the partial molar volume of pure water in the solution is equal to the molar volume of pure water. Since the hygroscopic diameter growth factor measurements are on volume basis using nano-HTDMA system, the expression of G_f as a function of molar ratio (x_j), molar mass (M_j), and mass density (ρ_j) of components j as follows:

$$G_f = \left[\frac{\sum_j\left(x_j M_j \frac{1}{\rho_j}\right)}{\sum_{j,j\neq w}\left(x_j M_j \frac{1}{\rho_j}\right)}\right]^{\frac{1}{3}} \quad (5)$$

2.2.3.2 Growth factor prediction by E-AIM model

The hygroscopic growth curve of aerosol particles is commonly evaluated from Extend-Aerosol Inorganic Model (E-AIM). It is a thermodynamic equilibrium model used for calculating phase partitioning (gas/liquid/solid). Most importantly, the E-AIM mode can model thermodynamic

https://doi.org/10.5194/acp-2022-544
Preprint. Discussion started: 22 August 2022


Atmospheric Chemistry and Physics Discussions

properties (e.g., water activity, liquid-vapor interfacial energy, and solution density) in the highly supersaturated concentration solution (Dutcher et al., 2013). Also, the standard universal quasi-chemical functional group activity coefficients (UNIFAC) within E-AIM can be used to predict a_w, σ_{sol}, and ρ_{sol} of organic aqueous solution (Fredenslund et al., 1975; Hansen et al., 1991). Note that, The E-AIM calculations based on the standard UNIFAC group contribution method are to predict hygroscopic growth factors of organic aerosol particles. (i.e.., E-AIM model (standard UNIFAC)) growth curve as a function of RH is based on Eq. (1) and Eq. (6).).

$$G_f = \left(\frac{\rho_s}{x_s \rho_{sol}}\right)^{\frac{1}{3}} \quad (6)$$

ρ_s and ρ_{sol} are the density of solute and solution, respectively, and x_s is the solute mass fraction.

2.2.4 Calculation of ratio of gas-phase concentration to the total concentration

2.2.4.1 Calculation of gas-phase concentration (g/cm^3)

$$P_A = P_A^0 exp\left(\frac{2\sigma M}{RT\rho_l R_p}\right) \quad (7)$$

$$m_{gas} = \frac{PVM}{RT} \quad (8)$$

where P_A and P_A^0 are vapor pressure, equilibrium vapor pressure, respectively. σ, M, $\rho_l, and\ R_p$ mean surface tension, molecular weight of the substance, liquid-phase density, and a droplet of radius, respectively. This equation (Eq. 8) establish a relationship between mass in gas phase (m_{gas}) and pressure (P), volume (V), mole mass (M), the ideal gas constant (R), and temperature. Here, Vapor pressure (P) is equal to saturated ratio of levoglucosan vapor multiplied saturated levoglucosan vapor pressure at 293.15 K.

2.2.4.2 Calculation of total concentration of generated particles (g/cm^3)

https://doi.org/10.5194/acp-2022-544
Preprint. Discussion started: 22 August 2022


Atmospheric Chemistry and Physics Discussions

$$m_{total} = \frac{dN}{dlogD_p} \times dlogD_p \times \frac{\pi}{6} D_p^3 \times \rho \quad (9)$$

where dN is particle concentration, D_p is the particle diameter, and ρ is the density of particles.

2.2.4.3 Ratio of the gas-phase concentration to the total concentration of generated particles

$$Ratio = \frac{m_{gas}}{m_{total}} \quad (10)$$

3 Results and discussion

3.1 Levoglucosan

3.1.1 Concentration-dependent water activity of levoglucosan solution

Figure 2 shows KD-derived water activity of aqueous levoglucosan nanoparticles with molality up to 140 mol kg^{-1}. Here, by applying a water activity parameterization model (KD, Eq. 3) to measured growth factors of levoglucosan aerosol nanoparticles with diameters from 20 to 100 nm using a nano-HTDMA. Chan et al. (2005) levitated single particles of ~10 μm levoglucosan at the different RHs in an electrodynamic balance for mass measurements, and reported water activity data for aqueous droplets with molality up to 14 mol kg^{-1}. These water activity data are compared with predictions from the Köhler (Kreidenweis et al., 2005, Eq. 2) and the E-AIM model, respectively. A good agreement between KD-derived water activity and Köhler indicates these aerosol particles are diluted aqueous droplets with molality less than 20 mol kg^{-1}. However, a derivation of Köhler from the KD-derived water activity is observed as the molality increases from 20 to 120 mol kg^{-1}, indicating levoglucosan nanoparticles become the highly supersaturated. Also, a discrepancy exists between KD-derived data and E-AIM model prediction. For DKA-derived water activity calculations, a strong size dependence of the hygroscopic growth factors is needed for aerosol

https://doi.org/10.5194/acp-2022-544
Preprint. Discussion started: 22 August 2022


Atmospheric Chemistry and Physics Discussions

nanoparticles in the different sizes, which is not the case for the hygroscopic measurements of levoglucosan nanoparticles.

3.1.2 Size dependent hygroscopicity of levoglucosan nanoparticles

Black solid squares in Fig. 3 shows the measured humidogram of 100-nm levoglucosan nanoparticles in both deliquescence and efflorescence modes. Levoglucosan nanoparticles uptake water continuously from 5 % to 90 % RH. Also, they gradually release water as RH decreases down to 5 %. The hygroscopic growth factors of levoglucosan nanoparticles in deliquescence and efflorescence modes overlap. For example, the hygroscopic growth factors of levoglucosan nanoparticles at 80 % RH, 87 % RH are 1.16, 1.23, respectively, in the deliquescence mode, very close to the corresponding values in the efflorescence mode are 1.15, 1.22 (shown in Fig. S1), suggesting that growing and shrinking of particles are in equilibrium with water vapor surrounding moisture conditions. No prompt phase transitions of levoglucosan nanoparticles are observed in both deliquescence and efflorescence modes. A similar non-prompt phase transition of levoglucosan nanoparticles was observed in the previous studies (Mochida and Kawamura, 2004; Chan et al., 2005; Svenningsson et al., 2006; Mikhailov et al., 2008; Lei et al., 2014, 2018). This study is in good agreement with most of reference results, but there is a difference in the hygroscopic growth factor of levoglucosan nanoparticles between Mikhailov et al. (2008) and this study. The reason is that Mikhailov et al. (2008) used minimum mobility diameter measured in the hydration and dehydration modes instead of the initial dry mobility diameter measured in the hydration or dehydration modes to calculate the hygroscopic growth factor of levoglucosan nanoparticles, which could lead to the higher hygroscopic growth factors of levoglucosan nanoparticles than that of this study.

https://doi.org/10.5194/acp-2022-544
Preprint. Discussion started: 22 August 2022


Atmospheric Chemistry and Physics Discussions

Figure 4 shows measured size-resolved hygroscopic growth factors of levoglucosan nanoparticles against RH up to 90 %. There is a weak size dependence of hygroscopic growth factors of levoglucosan nanoparticles with diameters down to 20 nm in both deliquescence and efflorescence modes. E.g., a slight difference in hygroscopic growth factor between 100 and 20-nm levoglucosan nanoparticles is ~0.02 at 88 % RH. In addition, E-AIM (standard UNIFAC) model and ideal solution theory are used to predict our measurement results as shown in Fig. 4a and 4b, respectively. E-AIM (standard UNIFAC) model is applied to estimate the hygroscopic growth of organic aerosol nanoparticles according to UNIFAC group contribution method. Ideal solution theory is used to describe water absorption of the ideal/diluted aqueous solution nanodroplets. Due to consideration of Kelvin effect in model and theory, these model predictions are expected to present a size dependence of growth factors of nanoparticles in size from 100 down to 20 nm. For example, as shown in Fig. 4a, the thermodynamic equilibrium model (E-AIM (standard UNIFAC)) shows a weak size dependence of the growth factors of levoglucosan nanoparticles with diameters 100, 60, and 20 nm at low RH but a strong size dependence of growth factors at RH above 70 %. However, the calculated growth factors of nanoparticles down to 20 nm in size are deviated from the measured growth factors of levoglucosan nanoparticles at RH below 80 %, which is similar to the observation of 100-nm levoglucosan hygroscopicity prediction from previous studies (Lei et al., 2014, 2018). Lei et al. (2014, 2018) explained that the possible reason for this discrepancy is that the E-AIM (standard UNIFAC) predictions are not suitable for organic compounds with the strongly polar functional groups in series (Fredenslund et al., 1975; Hansen et al., 1991). Since levoglucosan contains three OH groups in series, thus, thermodynamic properties (e.g., water activity, surface tension) in E-AIM (standard UNIFAC) are more likely to be invalid for levoglucosan system. However, a good agreement of growth factors of levoglucosan with

https://doi.org/10.5194/acp-2022-544
Preprint. Discussion started: 22 August 2022

Atmospheric Chemistry and Physics Discussions

diameters 100, 60, and 20 nm is observed between measurements and predictions by ideal solution theory as shown in Fig. 4b.

The hygroscopic growth for sub-20 nm levoglucosan nanoparticles cannot be determined with the nano-HTDMA system because we observed significant evaporation of the dry particles in the measurement system. Figure 5a-b shows the measured peak diameter of normalized size distribution scanned by the nano-DMA2 and nano-DMA1 for sub-20 nm levoglucosan nanoparticles. It is obvious that the size of nanoparticles in DMA2 is smaller than that in DMA1, corresponding to a decrease of 22% to 50% of 15-nm and 10-nm levoglucosan nanoparticles, respectively, indicating significant evaporation of these small levoglucosan nanoparticles in the system. To test this hypothesis, we estimate the ratio of gas-phase concentration to the total concentration of the generated levoglucosan nanoparticles in the different sizes. Firstly, the calculated gas-phase concentration of levoglucosan is based on the Kelvin equation and ideal gas equation (Eq. 7&8, Sect. 2.2.4). Figure 5c shows the vapor saturation ratio of levoglucosan as nanodroplet diameter increases from 0 to 100 nm. The inset in Fig. 5c is an enlarged view (black open square) of vapor saturation ratio of levoglucosan as a function of nanodroplet diameters below 20 nm. The Kelvin effect on levoglucosan nanodroplets is very weak at diameters above 20 nm, but significantly enhanced for levoglucosan nanodroplets with diameters below 20 nm. Secondly, the total concentration of levoglucosan particles is estimated by Eq. (9). Thus, the results of the ratio of gas-phase concentration (m_g) to the total concentration (m_t) have been shown in Fig. 5d and Table S3 for levoglucosan nanoparticles in the diameter range from 10 to 100 nm. It shows a slight increase in the calculated ratio (m_g/m_t) for levoglucosan aerosol nanoparticles with dimeters from 100 down to 20 nm. However, the ratio of gas-phase concentration to the total concentration is dramatically enhanced for sub-20 nm levoglucosan aerosol nanoparticles, which is consistent with

https://doi.org/10.5194/acp-2022-544
Preprint. Discussion started: 22 August 2022


Atmospheric Chemistry and Physics Discussions

308 measurement observations, indicting the larger impact of evaporation of sub-20 nm levoglucosan
309 nanoparticles on the measurement results.

310 **3.2 D-glucose**

311 **3.2.1 Concentration-dependent water activity of D-glucose solution**

312 Figure 6 shows the DKA-derived water activity of aqueous D-glucose nanodroplets with diameters
313 from 6 nm to 100 nm with molality up to 1000 mol kg^{-1} (Cheng et al., 2015, Eq. 4). Here, by
314 comparing with KD-derived water activity, Köhler, E-AIM model, and observation from literatures
315 (Comesaña et al., 2001; Peng et al., 2001; Bhandari and Bareyre, 2003; Ferreira et al., 2003), a
316 good agreement between them is observed in the solute concentration below 20 mol kg^{-1}. However,
317 there is a disagreement between water activity results in the highly supersaturated concentration
318 range (> 20 mol kg^{-1}).

319 **3.2.2 Size dependent hygroscopicity of D-glucose nanoparticles**

320 Figure 7 shows the measured hygroscopic growth factors of 100-nm D-glucose nanoparticles as a
321 function of RH. No significant difference in the hygroscopic growth factor of 100-nm D-glucose
322 nanoparticles is found between deliquescence and efflorescence measurement modes (Fig. S2). For
323 example, the measured growth factors of D-glucose nanoparticles at 81 % RH, 88 % RH are 1.16,
324 1.25 in the deliquescence mode, respectively, in good agreement with results in the efflorescence
325 mode (g_f=1.17 at 81 % RH, g_f=1.26 at 88 % RH shown in Fig. S2). Also, measured hygroscopic
326 growth factors of 100-nm D-glucose are consistent with results from previous studies (Mochida
327 and Kawamura. 2004; Suda and Petters, 2013; Estillore et al., 2017; Mikhailov and Vlasenko,
328 2020). No prompt phase transitions are observed during in both deliquescence and efflorescence
329 measurement modes. Estillore et al. (2017) observed a slightly amorphous structure of D-glucose

https://doi.org/10.5194/acp-2022-544
Preprint. Discussion started: 22 August 2022


Atmospheric Chemistry and Physics Discussions

particles under ambient conditions using an atomic force microscopy and D-glucose particles grow through gradual water uptake where the solid-liquid phase transition is non-discrete. Thus, a continuous growth/shrink of diameter in both deliquescence and efflorescence modes is explained by the lack of crystallization of D-glucose nanoparticles upon drying to low RH below 10%.

Figure 8a shows the size dependence of measured hygroscopic growth factors of D-glucose nanoparticles in the size range from 6 to 100 nm, with differences in growth factor up to 0.14 between 100-nm and 6-nm nanoparticles at 90 % RH (Fig. S2). A weak size dependence on the hygroscopic growth factors of D-glucose nanoparticles is observed in the size range from 20 to 100 nm, which is similar to observation for levoglucosan nanoparticles with diameters down to 20 nm. However, there is a strong size-dependent growth factor of D-glucose nanoparticles with diameters from 6 to 20 nm, especially at high RH, i.e., RH > ~80%. There is no evident difference in hygroscopic growth factors of D-glucose nanoparticles at RH below 80 % in size range from 6 to 100 nm. To have a clear observation for size dependence of the hygroscopic growth factor of D-glucose aerosol nanoparticles with diameters down to 6 nm, Fig. 8b shows the change in the hygroscopic growth factor of D-glucose aerosol nanoparticles with diameters from 100 down to 6 nm at 87 % RH. The hygroscopic growth factor of D-glucose nanoparticles is almost unchanged with diameters from 20 to 100 nm. However, a markedly increase in the hygroscopic growth factor of D-glucose aerosol nanoparticles is observed as size increases from 6 to 20 nm. E-AIM model predict well the measured hygroscopic growth factors of D-glucose with diameters smaller than 15 nm at 87 % RH, while ideal solution theory agrees with hygroscopic measurement results of D-glucose with diameters higher than 60 nm at the same RH. The use of DKA methods leads to a good agreement between measurements and model predictions.

https://doi.org/10.5194/acp-2022-544
Preprint. Discussion started: 22 August 2022


Atmospheric Chemistry and Physics Discussions

352 The measured hygroscopic growth factors of D-glucose nanoparticles with diameters of 6 and 100
353 nm are compared with the model and theory shown in Fig. 9, Fig. S3, and Fig. S4, respectively.
354 Note that, E-AIM (standard UNIFAC) model prediction is optimized for organic compounds with
355 lesser polar groups in series, i.e., intramolecular interaction, such as hydrogen bond between polar
356 groups, may result in model prediction inaccuracy. Ideal solution theory is applied to predict the
357 hygroscopic growth factor of organics in the ideal solution. Figure 9a and Fig. S3 show that the
358 measured growth factors of 100-nm D-glucose nanoparticles are lower than predicted growth
359 factors from E-AIM (standard UNIFAC) model, especially at RH below 85 %. Also, E-AIM
360 (standard UNIFAC) model could predict well the measured hygroscopic growth factor of 6-nm D-
361 glucose aerosol nanoparticles at RH above 40 % shown in Fig. 9a and Fig. S3. The possible reason
362 for discrepancies between E-AIM (standard UNIFAC) model and measurements is inaccurate
363 thermodynamic parameters (e.g., water activity, surface tension) estimated by the E-AIM (standard
364 UNIFAC) model without consideration intramolecular interaction. D-glucose contains five OH
365 groups in series, hydrogen bond could potentially exist and affects the E-AIM (standard UNIFAC)
366 model-measurement agreement for D-glucose aerosol nanoparticles system. Using ideal solution
367 theory is to predict the hygroscopic curve of D-glucose nanoparticles with diameters of 6-100 nm
368 shown in Fig. 9b and Fig. S3. There is a good agreement between measured growth factors of 100-
369 nm D-glucose and ideal theory predictions. This suggests that thermodynamic parameters (e.g.,
370 water activity, surface tension, and solution density) assumed by the ideal solution theory are
371 accurate to use in Eq. (1) and (2) for predicting the hygroscopic curve of D-glucose nanoparticles
372 with large sizes (e.g., 60, 100 nm). However, an underestimation of growth factors of 6-nm D-
373 glucose nanoparticles has been shown in Fig. 9b and Fig. S3 by ideal solution theory prediction at
374 RH above 30 %. The possible reason is the unfavorable assumption of ideal solution theory. As D-
375 glucose size decreases from 20 to 6 nm, D-glucose nanodroplets could be highly supersaturated in

https://doi.org/10.5194/acp-2022-544
Preprint. Discussion started: 22 August 2022


Atmospheric Chemistry and Physics Discussions

concentration compared to the dilution solution. However, the current thermodynamic models (e,g., E-AIM) mostly rely on the concentration-dependent thermodynamic properties (such as water activity) derived from the measurements of large aerosol particles or even bulk samples (Tang and Munkelwitz, 1994; Tang, 1996; Pruppacher and Klett, 1997; Clegg et al., 1998). They are thus difficult or impossible to apply to describe the hygroscopic behavior of sub-10 nm nanoparticles, which can often be supersaturated in concentration compared to bulk solutions (Cheng et al., 2015; Wang et al., 2018). Thus, nanosize effect on these thermodynamic properties have been taken into account in the models and theories (Cheng et al., 2015). Combination of DKA methods and hygroscopic measurements of aerosol nanoparticles in the different sizes can use to determine the thermodynamic properties (e.g., water activity) in the highly supersaturated concentration range (Cheng et al., 2015). Therefore, as shown in Fig. 9c and Fig. S4, the use of the DKA method leads a good agreement with the measured hygroscopic growth factors of Glucose nanoparticles with diameters from 100 down to 6 nm.

4 Conclusions

In this study, we investigate the hygroscopic behavior of levoglucosan and D-glucose nanoparticles with diameters down to 6 nm using a nano-HTDMA. Due to the larger impact of evaporation of sub-20 nm levoglucosan nanoparticles in the nano-HTDMA system, we measure hygroscopic growth factor of levoglucosan with diameters down to 20 nm. There is a weak size dependence of hygroscopic growth factor of levoglucosan and D-glucose with diameters down to 20 nm, while a strong size dependence of the hygroscopic growth factor of D-glucose has been clearly observed in the size range from 6 to 20 nm. No prompt phase transitions occur in both deliquescence and efflorescence modes for both levoglucosan and D-glucose nanoparticles. By comparing with the

https://doi.org/10.5194/acp-2022-544
Preprint. Discussion started: 22 August 2022


Atmospheric Chemistry and Physics Discussions

KD-derived water activity, Köhler, E-AIM model, and DKA-derived data, the predicted water activity of aqueous organic solution (levoglucosan and D-glucose) is consistent with observation data from references in the low solute concentration (< 20 mol kg^{-1}) but failed in the solute concentration (> 20 mol kg^{-1}). In addition, ideal solution theory predicts well the hygroscopic behavior of two specific organics with diameters higher than 60 nm (levoglucosan and D-glucose), while hygroscopic growth factor of D-glucose down to 6 nm in size is in good agreement with E-AIM (standard UNIFAC) model prediction at high RH. The use of the DKA method leads to a good agreement with measured hygroscopic growth factor of glucose nanoparticles with diameters from 100 down to 6 nm.

Biomass burning is an important source of anthropogenic atmospheric aerosols. Aerosol particles in the biomass burning smoke enriched with hygroscopic behavior are suggested to act as efficient CCN. It is well known that aerosol population can appear as externally mixed or internally mixed (homogeneously internally, core-shell internally) in the biomass burning processes. The mixing structure has an important effect on the hygroscopic behavior of aerosol particles, especially for sub-100 nm size range. We will be able to investigate the effect of the mixing state on the hygroscopic behavior of aerosol nanoparticles from biomass burning in different sizes. This will further help us to understand their interaction with water vapor.

Data availability

Reader who are interested in the data should contact Yafang Cheng (Yafang.cheng@mpic.de).

Competing interests

https://doi.org/10.5194/acp-2022-544
Preprint. Discussion started: 22 August 2022


Atmospheric Chemistry and Physics Discussions

Some authors are members of the editorial board of journal Atmospheric Chemistry Physics. The peer-review process was guided by an independent editor, and the authors have also no other competing interests to declare

Acknowledgement

This study was supported by the Max Planck Society (MPG) and Leibniz Society. T.L acknowledges the support from China Scholarship Council (CSC). Y. C. would like to acknowledge the Minerva Program of MPG.

Author contributions: Y.C. and H.S. designed and led the study. T.L. performed the experiments. All co-authors discussed the results and commented on the manuscript. T.L. wrote the manuscript with input from all co-authors

4 References

Andreae, M. O. and Gelencsér, A.: Black carbon or brown carbon? The nature of light-absorbing carbonaceous aerosols, Atmos. Chem. Phys., 6, 3131–3148, https://doi.org/10.5194/acp-6-3131-2006, 2006.

Bhandari, B. and Bareyre, I.: Estimation of crystalline phase present in the glucose crystal–solution mixture by water activity measurement, LWT - Food Science and Technology, 36, 729-733, 2003.

Bhattarai, H., Saikawa, E., Wan, X., Zhu, H., Ram, K., Gao, S., Kang, S., Zhang, Q., Zhang, Y., Wu, G., Wang, X., Kawamura, K., Fu, P., and Cong, Z.: Levoglucosan as a tracer of biomass burning: Recent progress and perspectives, Atmos. Res., 220, 20–33, 2019.

https://doi.org/10.5194/acp-2022-544
Preprint. Discussion started: 22 August 2022

441 Biskos, G., Malinowski, A., Russell, L. M., Buseck, P. R., and Martin, S. T.: Nanosize effect on
442 the deliquescence and the efflorescence of sodium chloride particles, Aerosol Sci. Technol.,
443 40, 97-106, 2006a.
444 Biskos, G., Paulsen, D., Russell, L. M., Buseck, P. R., and Martin, S. T.: Prompt deliquescence and
445 efflorescence of aerosol nanoparticles, Atmos. Chem. Phys., 6, 4633–4642,
446 https://doi.org/10.5194/acp-6-4633-2006, 2006b.
447 Biskos, G., Russell, L. M., Buseck, P. R., and Martin, S. T.: Nanosize effect on the hygroscopic
448 growth factor of aerosol particles, Geophys. Res. Lett., 33, L07801,
449 doi:10.1029/2005GL025199, 2007.
450 Bohren, C. and Huffmann, D.: Absorption and scattering of light by small particles, Wiley-VCH,
451 New York, USA, 2004.
452 Bzdek, B. R., Zordan, C. A., Luther, G. W., and Johnston, M. V.: Nanoparticle Chemical
453 Composition During New Particle Formation, Aerosol Science and Technology, 45, 1041-
454 1048, 2011.
455 Chan, M. N., Choi, M. Y., Ng, N. L., and Chan, C. K.: Hygroscopicity of water-soluble organic
456 compounds in atmospheric aerosols: Amino acids and biomass burning derived organic species,
457 Environ. Sci. Technol., 39, 1555-1562, 2005.
458 Chan, M. N. C. a. C. K.: Mass transfer effects in hygroscopic measurements of aerosol particles,
459 Atmos. Chem. Phys., 5, 2703–2712, https://doi.org/10.5194/acp-5-2703-2005, 2005.
460 Charlson, R. J., Schwartz, S. E., Hales, J. M., Cess, R. D., Coakley, J. A., Hansen, J. E., and
461 Hoffmann, D. J.: Climate forcing by anthropogenic aerosols, Science, 255, 423-430, 1992.
462 Chen, Da-Ren, David Y.H. Pui, and Stanley L. Kaufman.: Electrospraying of conducting liquids
463 for monodisperse aerosol generation in the 4 nm to 1.8 nm diameter range, J. Aerosol Sci.,
464 26:963-977.

https://doi.org/10.5194/acp-2022-544
Preprint. Discussion started: 22 August 2022

465 Cheng, Y. F., Su, H., Koop, T., Mikhailov, E., and Pöschl, U.: Size dependence of phase transitions
466 in aerosol nanoparticles, Nat. Commun., 6, 5923, doi:10.1038/ncomms6923, 2015.
467 Cheng, Y. F., Su, H., Rose, D., Gunthe, S. S., Berghof, M., Wehner, B., Achtert, P., Nowak, A.,
468 Takegawa, N., Kondo, Y., Shiraiwa, M., Gong, Y. G., Shao, M., Hu, M., Zhu, T., Zhang, Y.
469 H., Carmichael, G. R., Wiedensohler, A., Andreae, M. O., and Pöschl, U.: Size-resolved
470 measurement of the mixing state of soot in the megacity Beijing, China: diurnal cycle, aging
471 and parameterization, Atmos. Chem. Phys., 12, 4477–4491, https://doi.org/10.5194/acp-12-
472 4477-2012, 2012.
473 Chýlek, P. and Coakley, J. A.: Aerosols and climate, Science, 183, 75-77, 1974.
474 Clegg, S. L., Brimblecombe, P., and Wexler, A. S.: Thermodynamic model of the system
475 H^+–NH_4^+–SO_4^{2-}–NO^{3-}–H_2O at tropospheric temperatures, J. Phys. Chem. A, 102, 2137–2154,
476 doi:10.1021/Jp973042r, 1998.
477 Clegg, S. L., Seinfeld, J. H., and Brimblecombe, P.: Thermody-namic modelling of aqueous
478 aerosols containing electrolytes and dissolved organic compounds, J. Aerosol Sci., 32, 713–
479 738, doi:10.1016/s0021-8502(00)00105-1, 2001.
480 Clegg, S. L. and Seinfeld, J. H.: Thermodynamic models of aqueous solutions containing in-
481 organic electrolytes and dicarboxylic acids at 298.15 K. 2. Systems including dissociation
482 equilibria, J. Phys. Chem. A, 110, 5718–5734, doi:10.1021/jp056150j, 2006.
483 Comesaña, J. F., Correa, A., and Sereno, A. M.: Water activity at 35 °C in 'sugar' + water and
484 'sugar' + sodium chloride + water systems, Int. J. Food Sci. Tech., 36, 655-661, 2001.
485 Dick, W. D., Saxena, P., and McMurry, P. H.: Estimation of water uptake by organic compounds
486 in submicron aerosols measured during the Southeastern Aerosol and Visibility Study, J. Geo-
487 phys. Res.-Atmos., 105, 1471–1479, doi:10.1029/1999jd901001, 2000.

https://doi.org/10.5194/acp-2022-544
Preprint. Discussion started: 22 August 2022

Atmospheric Chemistry and Physics Discussions

488 Dunne, E. M., Gordon, H., Kürten, A., Almeida, J., Duplissy, J., Williamson, C., Ortega, I. K.,
489 Pringle, K. J., Adamov, A., Baltensperger, U., Barmet, P., Benduhn, F., Bianchi, F.,
490 Breitenlechner, M., Clarke, A., Curtius, J., Dommen, J., Donahue, N. M., Ehrhart, S., Flagan,
491 R. C., Franchin, A., Guida, R., Hakala, J., Hansel, A., Heinritzi, M., Jokinen, T., Kangasluoma,
492 J., Kirkby, J., Kulmala, M., Kupc, A., Lawler, M. J., Lehtipalo, K., Makhmutov, V., Mann,
493 G., Mathot, S., Merikanto, J., Miettinen, P., Nenes, A., Onnela, A., Rap, A., Reddington, C.
494 L. S., Riccobono, F., Richards, N. A. D., Rissanen, M. P., Rondo, L., Sarnela, N.,
495 Schobesberger, S., Sengupta, K., Simon, M., Sipilä, M., Smith, J. N., Stozkhov, Y., Tomé, A.,
496 Tröstl, J., Wagner, P. E., Wimmer, D., Winkler, P. M., Worsnop, D. R., and Carslaw, K. S.:
497 Global atmospheric particle formation from CERN CLOUD measurements, Science., 354,
498 1119-1124, 2016.
499 Duplissy, J., Gysel, M., Sjogren, S., Meyer, N., Good, N., Kammermann, L., Michaud, V., Weigel,
500 R., Martins dos Santos, S., Gruening, C., Villani, P., Laj, P., Sellegri, K., Metzger, A.,
501 McFiggans, G. B., Wehrle, G., Richter, R., Dommen, J., Ristovski, Z., Baltensperger, U., and
502 Weingartner, E.: Intercomparison study of six HTDMAs: results and recommendations,
503 Atmos. Meas. Tech., 2, 363–378, https://doi.org/10.5194/amt-2-363-2009, 2009.
504 Dusek, U., Frank, G. P., Curtius, J., Drewnick, F., Schneider, J., Kürten, A., Rose, D., Andreae, M.
505 O., Borrmann, S., and Pöschl, U.: Enhanced organic mass fraction and decreased
506 hygroscopicity of cloud condensation nuclei (CCN) during new particle formation events,
507 Geophys. Res. Lett., 37, 2010.
508 Dutcher, C. S., Ge, X., Wexler, A. S. & Clegg, S. L. An Isotherm-Based Thermodynamic Model
509 of Multicomponent Aqueous Solutions, Applicable Over the Entire Concentration Range. J.
510 Phys. Chem. A 117, 3198-3213 (2013).

https://doi.org/10.5194/acp-2022-544
Preprint. Discussion started: 22 August 2022

Atmospheric Chemistry and Physics Discussions

511 Elias, V. O., Simoneit, B. R. T., Cordeiro, R. C., and Turcq, B.: Evaluating levoglucosan as an
512 indicator of biomass burning in Carajás, amazônia: a comparison to the charcoal
513 record22Associate editor: R. Summons, Geochim. Cosmochim. Acta., 65, 267-272, 2001.
514 Estillore, A. D., Morris, H. S., Or, V. W., Lee, H. D., Alves, M. R., Marciano, M. A., Laskina, O.,
515 Qin, Z., Tivanski, A. V., and Grassian, V. H.: Linking hygroscopicity and the surface
516 microstructure of model inorganic salts, simple and complex carbohydrates, and authentic sea
517 spray aerosol particles, Phys. Chem. Chem. Phys., 19, 21101-21111, 2017.
518 Ferreira, O., Brignole, E. A., and Macedo, E. A.: Phase equilibria in sugar solutions using the A-
519 UNIFAC model, Ind. Eng. Chem. Res., 42 (24), 6212–6222, 2003.
520 Fraser, M. P. and Lakshmanan, K.: Using Levoglucosan as a Molecular Marker for the Long-Range
521 Transport of Biomass Combustion Aerosols, Environ. Sci. Technol., 34, 4560-4564, 2000.
522 Fredenslund, A., Jones, R. L., and Prausnitz, J. M.: Group-contribution estimation of activity-
523 coefficients in nonideal liquid-mixtures, Aiche J., 21, 1086–1099, doi:10.1002/aic.690210607,
524 1975.
525 Hämeri, K., Laaksonen, A., Väkevä, M., and Suni, T.: Hygroscopic growth of ultrafine sodium
526 chloride particles, J. Geophys. Res., 106, 20 749–20 757, 2001.
527 Hämeri, K., Väkevä, M., Hansson, H.-C., and Laaksonen, A.: Hygroscopic growth of ultrafine
528 ammonium sulfate aerosol measured using an ultrafine tandem differential mobility analyzer,
529 J. Geophys. Res., 105, 22 231–22 242, 2000.
530 Hansen, H. K., Rasmussen, P., Fredenslund, A., Schiller, M., and Gmehling, J.: Vapor–liquid
531 equilibria by UNIFAC group contribution. 5. Revision and extension, Ind. Eng. Chem. Res.,
532 30, 2352–2355, doi:10.1021/ie00058a017, 1991.
533 Kerminen, V.-M.: The effects of particle chemical character and atmospheric processes on particle
534 hygroscopic properties, J. Aerosol Sci., 28, 121–132, 1997.

https://doi.org/10.5194/acp-2022-544
Preprint. Discussion started: 22 August 2022

Atmospheric Chemistry and Physics Discussions

535 Keskinen, H., Virtanen, A., Joutsensaari, J., Tsagkogeorgas, G., Duplissy, J., Schobesberger, S.,
536 Gysel, M., Riccobono, F., Slowik, J. G., Bianchi, F., Yli-Juuti, T., Lehtipalo, K., Rondo, L.,
537 Breitenlechner, M., Kupc, A., Almeida, J., Amorim, A., Dunne, E. M., Downard, A. J.,
538 Ehrhart, S., Franchin, A., Kajos, M. K., Kirkby, J., Kürten, A., Nieminen, T., Makhmutov, V.,
539 Mathot, S., Miettinen, P., Onnela, A., Petäjä, T., Praplan, A., Santos, F. D., Schallhart, S.,
540 Sipilä, M., Stozhkov, Y., Tomé, A., Vaattovaara, P., Wimmer, D., Prevot, A., Dommen, J.,
541 Donahue, N. M., Flagan, R. C., Weingartner, E., Viisanen, Y., Riipinen, I., Hansel, A., Curtius,
542 J., Kulmala, M., Worsnop, D. R., Baltensperger, U., Wex, H., Stratmann, F., and Laaksonen,
543 A.: Evolution of particle composition in CLOUD nucleation experiments, Atmos. Chem.
544 Phys., 13, 5587–5600, https://doi.org/10.5194/acp-13-5587-2013, 2013.
545 Kim, J., Ahlm, L., Yli-Juuti, T., Lawler, M., Keskinen, H., Tröstl, J., Schobesberger, S., Duplissy,
546 J., Amorim, A., Bianchi, F., Donahue, N. M., Flagan, R. C., Hakala, J., Heinritzi, M., Jokinen,
547 T., Kürten, A., Laaksonen, A., Lehtipalo, K., Miettinen, P., Petäjä, T., Rissanen, M. P., Rondo,
548 L., Sengupta, K., Simon, M., Tomé, A., Williamson, C., Wimmer, D., Winkler, P. M., Ehrhart,
549 S., Ye, P., Kirkby, J., Curtius, J., Baltensperger, U., Kulmala, M., Lehtinen, K. E. J., Smith, J.
550 N., Riipinen, I., and Virtanen, A.: Hygroscopicity of nanoparticles produced from
551 homogeneous nucleation in the CLOUD experiments, Atmos. Chem. Phys., 16, 293–304,
552 https://doi.org/10.5194/acp-16-293-2016, 2016.
553 Koehler, K. A., Kreidenweis, S. M., DeMott, P. J., Prenni, A. J., Carrico, C. M., Ervens, B., and
554 Feingold, G.: Water activity and activation diameters from hygroscopicity data - Part II:
555 Application to organic species, Atmos. Chem. Phys., 6, 795-809, 2006.
556 Köhler, H.: The nucleus in and the growth of hygroscopic droplets, Trans. Faraday Soc., 32, 1152–
557 1161, 1936.

https://doi.org/10.5194/acp-2022-544
Preprint. Discussion started: 22 August 2022

558 Kreidenweis, S. M., Koehler, K., DeMott, P. J., Prenni, A. J., Carrico, C., and Ervens, B.: Water
559 activity and activation diameters from hygroscopicity data - Part I: Theory and application to
560 inorganic salts, Atmos. Chem. Phys., 5, 1357–1370, https://doi.org/10.5194/acp-5-1357-2005,
561 2005.
562 Kulmala, M., Kontkanen, J., Junninen, H., Lehtipalo, K., Manninen, H. E., Nieminen, T., Petäjä,
563 T., Sipilä, M., Schobesberger, S., Rantala, P., Franchin, A., Jokinen, T., Järvinen, E., Äijälä,
564 M., Kangasluoma, J., Hakala, J., Aalto, P. P., Paasonen, P., Mikkilä, J., Vanhanen, J., Aalto,
565 J., Hakola, H., Makkonen, U., Ruuskanen, T., Mauldin, R. L., Duplissy, J., Vehkamäki, H.,
566 Bäck, J., Kortelainen, A., Riipinen, I., Kurtén, T., Johnston, M. V., Smith, J. N., Ehn, M.,
567 Mentel, T. F., Lehtinen, K. E. J., Laaksonen, A., Kerminen, V.-M., and Worsnop, D. R.: Direct
568 Observations of Atmospheric Aerosol Nucleation, Science, 339, 943-946, 2013.
569 Lei, T., Ma, N., Hong, J., Tuch, T., Wang, X., Wang, Z., Pöhlker, M., Ge, M., Wang, W., Mikhailov,
570 E., Hoffmann, T., Pöschl, U., Su, H., Wiedensohler, A., and Cheng, Y.: Nano-hygroscopicity
571 tandem differential mobility analyzer (nano-HTDMA) for investigating hygroscopic
572 properties of sub-10 nm aerosol nanoparticles, Atmos. Meas. Tech., 13, 5551–5567,
573 https://doi.org/10.5194/amt-13-5551-2020, 2020
574 Lei, T., Zuend, A., Cheng, Y., Su, H., Wang, W., and Ge, M.: Hygroscopicity of organic surrogate
575 compounds from biomass burning and their effect on the efflorescence of ammonium
576 sulfate in mixed aerosol particles, Atmos. Chem. Phys., 18, 1045-1064, 2018.
577 Lei, T., Zuend, A., Wang, W. G., Zhang, Y. H., and Ge, M. F.: Hygroscopicity of organic
578 compounds from biomass burning and their influence on the water uptake of mixed organic
579 ammonium sulfate aerosols, Atmos. Chem. Phys., 14, 11165-11183, 2014.
580 Lihavainen, H., Kerminen, V.-M., Komppula, M., Hatakka, J., Aaltonen, V., Kulmala, M., and
581 Viisanen, Y.: Production of "potential" cloud condensation nuclei associated with

https://doi.org/10.5194/acp-2022-544
Preprint. Discussion started: 22 August 2022

582 atmospheric new-particle formation in northern Finland, J. Geophys. Res., 108, 4782,
583 doi:10.1029/2003JD003887, 2003.
584 Mikhailov, E., Vlasenko, S., Martin, S. T., Koop, T., and Pöschl, U.: Amorphous and crystalline
585 aerosol particles interacting with water vapor: conceptual framework and experimental
586 evidence for restructuring, phase transitions and kinetic limitations, Atmos. Chem. Phys., 9,
587 9491–9522, https://doi.org/10.5194/acp-9-9491-2009, 2009.
588 Mikhailov, E. F. and Vlasenko, S. S.: High humidity tandem differential mobility analyzer for
589 accurate determination of aerosol hygroscopic growth, microstructure and activity
590 coefficients over a wide range of relative humidity, Atmos. Meas. Tech., 13, 2035–2056,
591 https://doi.org/10.5194/amt-13-2035-2020, 2020.
592 Mikhailov, E. F., Vlasenko, S. S., and Ryshkevich, T. I.: Influence of chemical composition and
593 microstructure on the hygroscopic growth of pyrogenic aerosol, Izv. Atmos. Ocean. Phy., 44,
594 416–431, 2008.
595 Mochida, M. and Kawamura, K.: Hygroscopic properties of levoglucosan and related organic
596 compounds characteristic to biomass burning aerosol particles, J. Geophys. Res.-Atmos., 109,
597 D21202, doi:10.1029/2004jd004962, 2004.
598 Peng, C., Chow, A. H. L., and Chan, C. K.: Hygroscopic study of glucose, citric acid, and sorbitol
599 using an electrodynamic balance: comparison with UNIFAC Predictions, Aerosol Sci.
600 Technol., 35 (3), 753–758, 2001.
601 Pruppacher, H. R. and Klett, J. D: Microphysics of clouds and precipitation, Kluwer Academic
602 Publishers, 1997.
603 Raoux, S., Rettner, C. T., Jordan-Sweet, J. L., Kellock, A. J., Topuria, T., Rice, P. M., and Miller,
604 D. C.: Direct observation of amorphous to crystalline phase transitions in nanoparticle arrays
605 of phase change materials, J. Appl. Phys., 102, 094305 (2007).

https://doi.org/10.5194/acp-2022-544
Preprint. Discussion started: 22 August 2022

606 Randles, C. A., Russell, L. M., and Ramaswamy, V.: Hygroscopic and optical properties of organic
607 sea salt aerosol and consequences for climate forcing, Geophys. Res. Lett., 31, L16 108,
608 doi:10.1029/2004GL020628, 2004.
609 Seinfeld, J. H., and Pandis, S. N.: Atmospheric Chemistry and Physics: From Air Pollution to
610 Climate Change (Second edition), Wiley Interscience, New York, 2006.
611 Sihto, S. L., Mikkilä, J., Vanhanen, J., Ehn, M., Liao, L., Lehtipalo, K., Aalto, P. P., Duplissy, J.,
612 Petäjä, T., Kerminen, V. M., Boy, M., and Kulmala, M.: Seasonal variation of CCN
613 concentrations and aerosol activation properties in boreal forest, Atmos. Chem. Phys., 11,
614 13269-13285, https://doi.org/10.5194/acp-11-13269-2011, 2011.
615 Simoneit, B. R. T., Schauer, J. J., Nolte, C. G., Oros, D. R., Elias, V. O., Fraser, M. P., Rogge, W.
616 F., and Cass, G. R.: Levoglucosan, a tracer for cellulose in biomass burning and atmospheric
617 particles, Atmos. Environ, 33, 173-182, 1999.
618 Suda, S. R. and Petters, M. D.: Accurate determination of aerosol activity coefficients at relative
619 humidities up to 99 % using the hygroscopicity tandem differential mobility analyzer
620 technique, Aerosol Sci. Technol., 47, 991–
621 1000, https://doi.org/10.1080/02786826.2013.807906, 2013.
622 Su, H., Rose, D., Cheng, Y. F., Gunthe, S. S., Massling, A., Stock, M., Wiedensohler, A., Andreae,
623 M. O., and Pöschl, U.: Hygroscopicity distribution concept for measurement data analysis and
624 modeling of aerosol particle mixing state with regard to hygroscopic growth and CCN
625 activation, Atmos. Chem. Phys., 10, 7489–7503, https://doi.org/10.5194/acp-10-7489-2010,
626 2010.
627 Svenningsson, B., Rissler, J., Swietlicki, E., Mircea, M., Bilde, M., Facchini, M. C., Decesari, S.,
628 Fuzzi, S., Zhou, J., Mønster, J., and Rosenørn, T.: Hygroscopic growth and critical

https://doi.org/10.5194/acp-2022-544
Preprint. Discussion started: 22 August 2022

supersaturations for mixed aerosol particles of inorganic and organic compounds of atmospheric relevance, Atmos. Chem. Phys., 6, 1937-1952, 2006.

Tang, I. N.: Chemical and size effects of hygroscopic aerosols on light scattering coefficients, J. Geophys. Res., 101, 19 245– 19 250, 1996.

Tang, I. N., Fung, K. H., Imre, D. G., and Munkelwitz, H. R.: Phase Transformation and Metastability of Hygroscopic Microparticles, J. Geophys. Res.-Atmos, 99, 18801– 18808, 1994.

Wang, J., Shilling, J. E., Liu, J., Zelenyuk, A., Bell, D. M., Petters, M. D., Thalman, R., Mei, F., Zaveri, R. A., and Zheng, G.: Cloud droplet activation of secondary organic aerosol is mainly controlled by molecular weight, not water solubility, Atmos. Chem. Phys., 19, 941-954, 2019.

Wang, Z., Cheng, Y., Ma, N., Mikhailov, E., Pöschl, U., and Su, H.: Dependence of the hygroscopicity parameter κ on particle size, humidity and solute concentration: implications for laboratory experiments, field measurements and model studies, Atmos. Chem. Phys. Discuss., 2017, 1-33, 2017.

Wang, Z., Su, H., Wang, X., Ma, N., Wiedensohler, A., Pöschl, U., and Cheng, Y.: Scanning supersaturation condensation particle counter applied as a nano-CCN counter for size-resolved analysis of the hygroscopicity and chemical composition of nanoparticles, Atmos. Meas. Tech., 8, 2161–2172, https://doi.org/10.5194/amt-8-2161-2015, 2015.

Wiedensohler, A., Cheng, Y. F., Nowak, A., Wehner, B., Achtert, P., Berghof, M., Birmili, W., Wu, Z. J., Hu, M., Zhu, T., Takegawa, N., Kita, K., Kondo, Y., Lou, S. R., Hofzumahaus, A., Holland, F., Wahner, A., Gunthe, S. S., Rose, D., Su, H., and Pöschl, U.: Rapid aerosol particle growth and increase of cloud condensation nucleus activity by secondary aerosol formation and condensation: A case study for regional air pollution in northeastern China, J. Geophys. Res.–Atmos., 114, doi:10.1029/2008JD010884, 2009.

https://doi.org/10.5194/acp-2022-544
Preprint. Discussion started: 22 August 2022

Atmospheric Chemistry and Physics Discussions

653 Wiedensohler, A., Lütkemeier, E., Feldpausch, M., & Helsper, C. (1986). Investigation of the
654 bipolar charge distribution at various gas conditions. J. Aerosol Sci., 17(3), 413–416.
655 https://doi.org/10.1016/0021-8502(86)90118-7.
656 Zhang, R.: Getting to the Critical Nucleus of Aerosol Formation, Science, 328, 1366-1367, 2010.
657 Zhang, R., Khalizov, A., Wang, L., Hu, M., and Xu, W.: Nucleation and Growth of Nanoparticles
658 in the Atmosphere, Chem. Re., 112, 1957-2011, 2012.
659 Zhang, R., Suh, I., Zhao, J., Zhang, D., Fortner, E. C., Tie, X., Molina, L. T., and Molina, M. J.:
660 Atmospheric New Particle Formation Enhanced by Organic Acids, Science, 304, 1487-1490,
661 2004.
662 Zieger, P., Fierz-Schmidhauser, R., Weingartner, E., and Baltensperger, U.: Effects of relative
663 humidity on aerosol light scattering: results from different European sites, Atmos. Chem.
664 Phys., 13, 10609–10631, https://doi.org/10.5194/acp-13-10609-2013, 2013.
665
666
667
668
669
670
671
672
673
674
675
676

https://doi.org/10.5194/acp-2022-544
Preprint. Discussion started: 22 August 2022

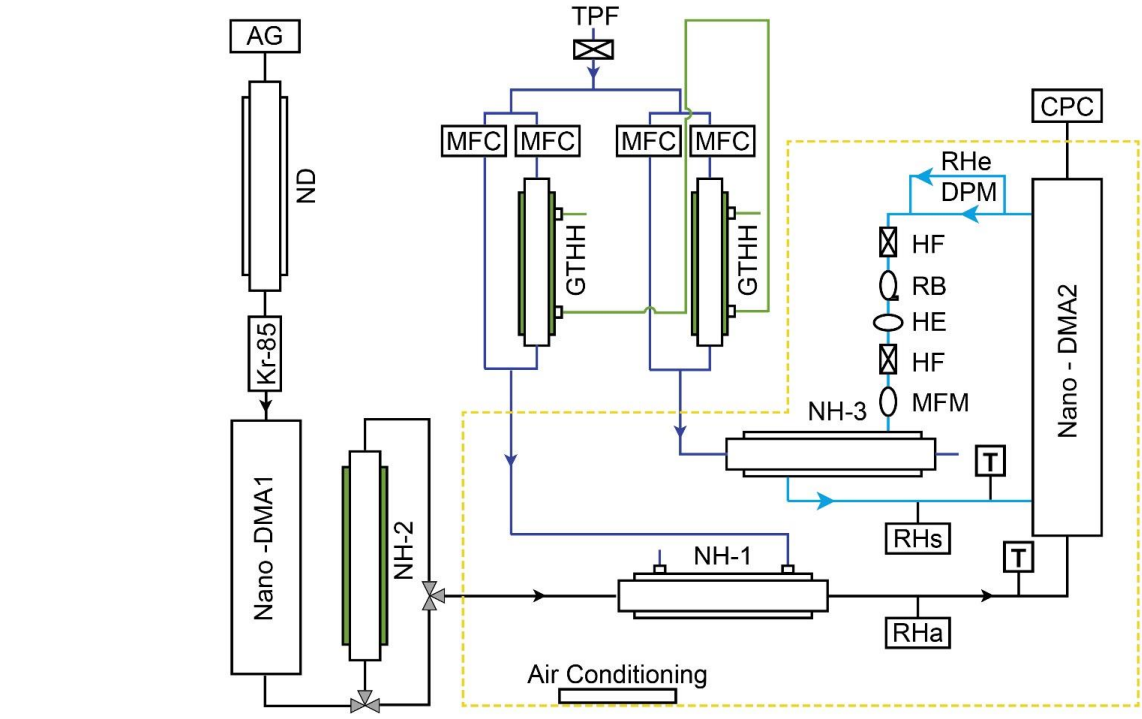

Figure 1. Experimental setup of the nano-HTDMA. Here, AG: aerosol generator (aerosol atomizer or electrospray); ND: nafion dryer; Kr-85: Krypton source aerosol neutralizer; Nano-DMA: nano differential mobility analyzer; TPF: total particle filter; HF: hydrophobic filter; MFC: mass flow controller; MFM: mass flow meter; RB: recirculation blower; DPM: dew point mirror; GTHH: Gore-Tex humidifier and heater; NH: nafion humidifier; HE: heat exchanger; CPC: condensation particle counter; Black line: aerosol line; Blue line: sheath line; Royal blue line: humidified air; Green line: MilliQ water (resistivity of 18.2 MΩ cm at 298.15 K). RH_a and RH_s (measured by RH sensors) represent the RH of aerosol and sheath flow in the inlet of nano-DMA2, respectively. RH_e (measured by dew point) represents the RH of excess air. T represent the temperature of aerosol and sheath flow in the inlet of nano-DMA2, respectively.

https://doi.org/10.5194/acp-2022-544
Preprint. Discussion started: 22 August 2022

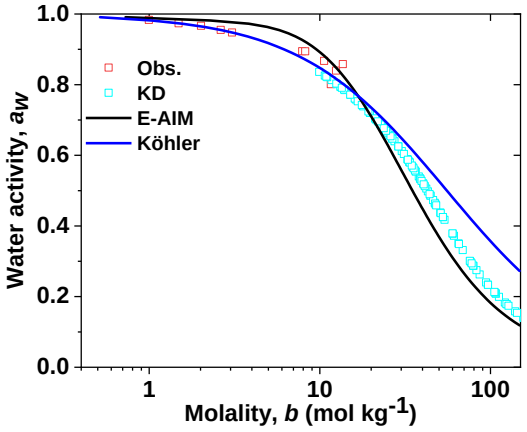

692

693 **Figure 2**. Concentration-dependent water activity (a_w) of levoglucosan solution. The KD-derived a_w (KD=Kreidenweis,
694 cyan open square) is compared with observations (red open square), E-AIM (Extend-Aerosol Inorganic Model, black
695 line), and a_w model (Köhler, blue line).

696

697

698

699

700

701

702

703

704

705

706

707

708

709

710

711

712

https://doi.org/10.5194/acp-2022-544
Preprint. Discussion started: 22 August 2022

Atmospheric Chemistry and Physics Discussions

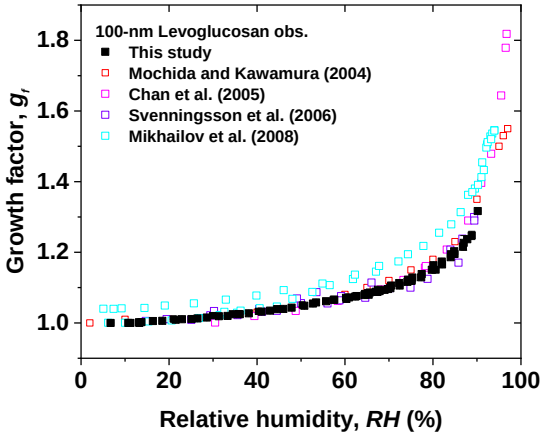

713

714 **Figure 3.** Hygroscopic diameter growth factor (G_f) of levoglucosan particles with dry diameter of 100 nm in both
715 deliquescence and efflorescence mode processes (black solid square). The measured data compared with literature data
716 from Mochida and Kawmura (2004) in both deliquescence and efflorescence modes (red open square), Chan et al.
717 (2005) in the deliquescence mode (magenta open square), Svenningsson et al. (2006) in the deliquescence mode (violet
718 open square), and Mikhailov et al. (2008) in both deliquescence and efflorescence modes (cyan open square).

719

720

721

722

723

724

725

726

727

https://doi.org/10.5194/acp-2022-544
Preprint. Discussion started: 22 August 2022

Atmospheric Chemistry and Physics Discussions

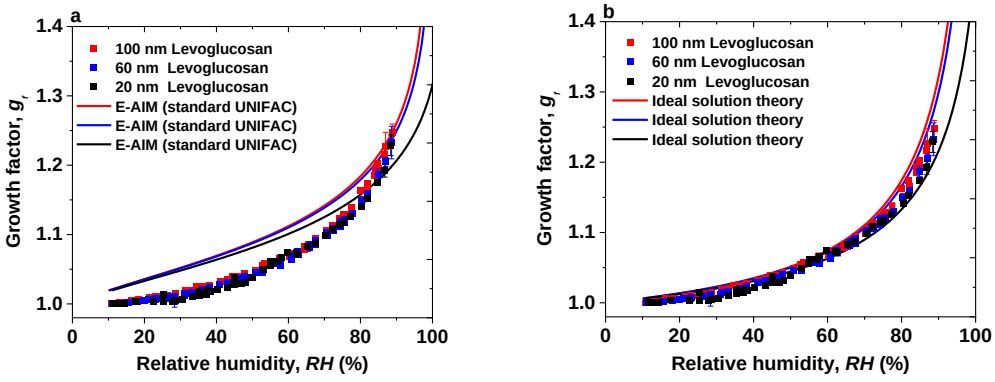

728

729 **Figure 4.** Hygroscopic diameter growth factor (G_f) of levoglucosan particles with dry diameter of 100 nm (red square),
730 60 nm (blue square), and 20nm (green square). Köhler model curves are based on: **(a)** E-AIM (standard UNIFAC)
731 (100 nm: red, 60 nm: blue, 20 nm: green line), **(b)** ideal solution theory (100 nm: red, 60 nm: blue, 20 nm: green line).

732

733

734

735

736

737

738

739

740

741

742

743

744

https://doi.org/10.5194/acp-2022-544
Preprint. Discussion started: 22 August 2022

Atmospheric Chemistry and Physics Discussions

745

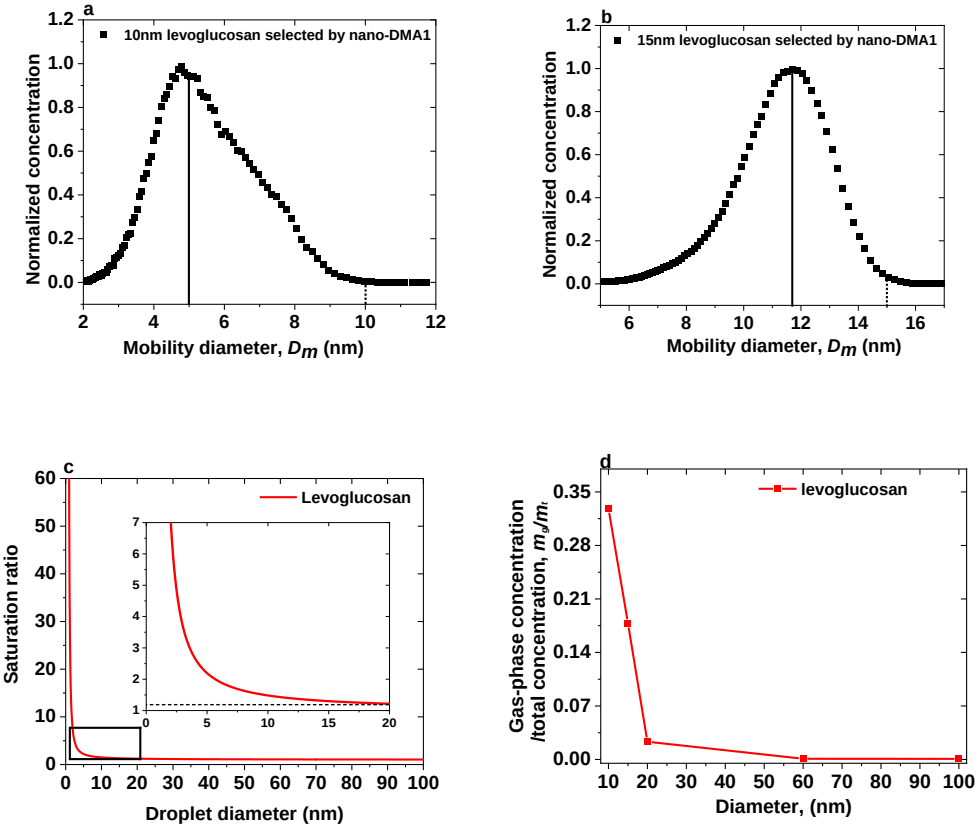

746

747 **Figure 5.** The normalized size distributions scanned by nano-DMA2 for: **(a)** 10 nm and **(b)** 15-nm levoglucosan at 10%
748 at 298K. The dotted lines mark the diameters of the monodispersed nanoparticles selected by the nano-DMA1. The
749 back solid lines mark the peak diameters from the normalized size distributions scanned by the nano-DMA2. **(c)** Vapor
750 saturation ratio of levoglucosan as a function of nanodroplet diameter according to the Kelvin equation. The diameter
751 range 0-20 nm for the saturation ratio of levoglucosan particles is shown as an inset. The value of surface tension of
752 pure levoglucosan is 0.0227104 [J m^{-2}]. **(d)** The ratio of gas-phase concentration (m_g) to the total concentration (m_t) of
753 levoglucosan nanoparticles against diameter.

754

755

756

757

https://doi.org/10.5194/acp-2022-544
Preprint. Discussion started: 22 August 2022

Atmospheric Chemistry and Physics Discussions

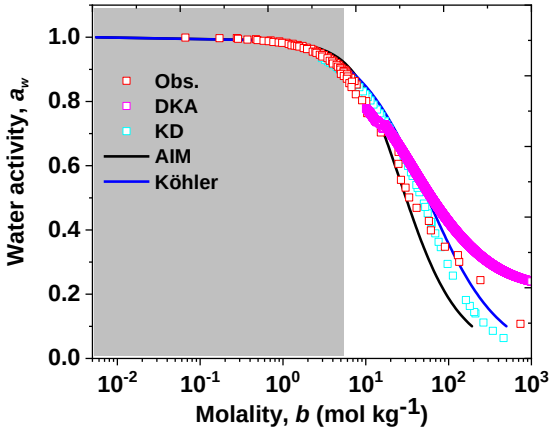

758

759 **Figure 6**. Concentration-dependent water activity (a_w) of levoglucosan solution. The DKA-derived a_w (Differential
760 Köhler Analysis, magenta open square) is compared with observations (red open square), E-AIM (Extend-Aerosol
761 Inorganic Model, black line), a_w model (Köhler, blue line), and parameterization model for a_w (KD=Kreidenweis, cyan
762 open square). The light grey shaded areas mark the sub-saturated concentration with respect to bulk solution.

763

764

765

766

767

768

769

770

771

https://doi.org/10.5194/acp-2022-544
Preprint. Discussion started: 22 August 2022

Atmospheric Chemistry and Physics Discussions

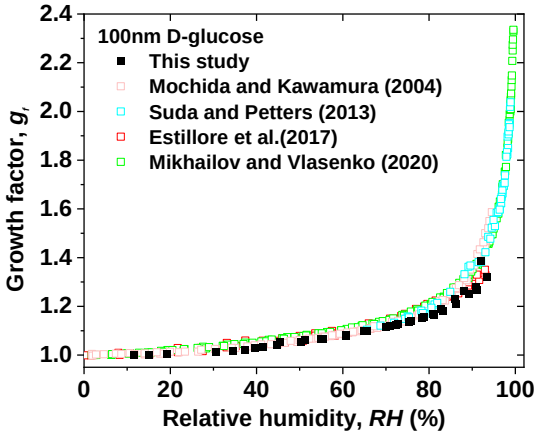

772

773 **Figure 7.** Hygroscopic diameter growth factor (G_f) of D-glucose particles with dry diameter of 100 nm in both
774 deliquescence and efflorescence modes (black solid square). The measured data compared with reference data from
775 Mochida and Kawmura (2004) in both deliquescence and efflorescence modes (pink open square), Suda and Petters,
776 (20017) in deliquescence mode (violet open square), Estillore et al., (2017) in both deliquescence and efflorescence
777 modes (red open square), and Mikhailov and Vlasenko (2020) in both deliquescence and efflorescence modes (green
778 open square).

779

780

781

782

783

784

785

786

787

https://doi.org/10.5194/acp-2022-544
Preprint. Discussion started: 22 August 2022

Atmospheric Chemistry and Physics Discussions

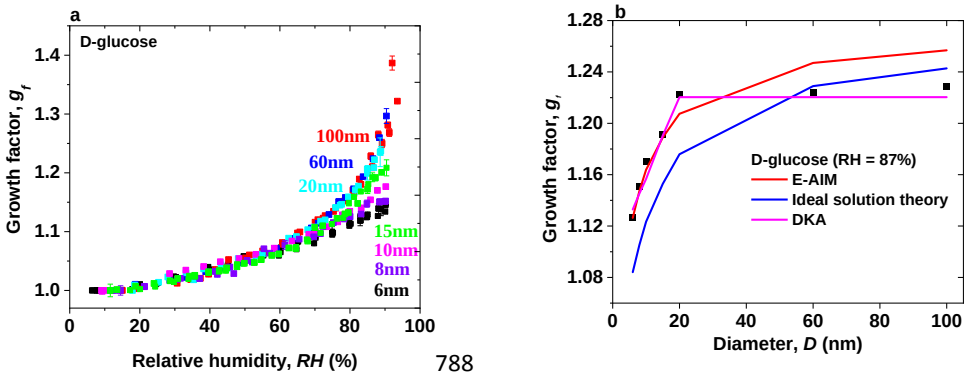

788

789 **Figure 8. (a)** Hygroscopic diameter growth factor (G_f) of D-glucose nanoparticles with dry diameters of 100 nm (red
790 square), 60 nm (blue square), 20 nm (cyan square), 15 nm (green square), 10 nm (pink square), 8 nm (royal square),
791 and 6 nm (black square). **(b)** Hygroscopic diameter growth factor (G_f, black square) of D-glucose nanoparticles with
792 dry diameters from 6 to 100 nm at 87% RH. The measured hygroscopic growth factors of D-glucose nanoparticles
793 with diameters from 100 down to are compared with E-AIM model (red line), ideal solution theory (blue line), and
794 DKA prediction (pink line).

795

796

797

798

799

800

801

802

803

804

https://doi.org/10.5194/acp-2022-544
Preprint. Discussion started: 22 August 2022

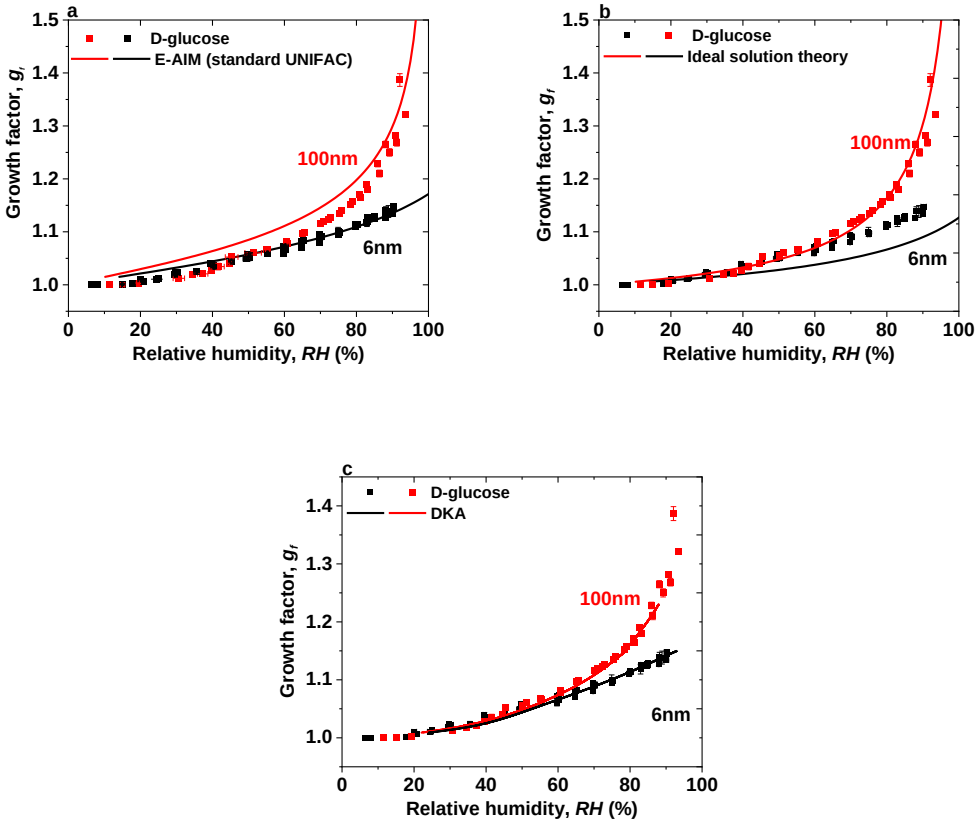

Figure 9. Hygroscopic diameter growth factor (G_f) of D-glucose nanoparticles with dry diameters of 100 nm (red square) and 6 nm (black square). Köhler model curves are based on: **(a)** AIM (standard UNIFAC), (100 nm: red, 6 nm: black line), **(b)** ideal solution theory (100 nm: red, 6 nm: black line), and **(c)** DKA mode (100 nm: red, 6 nm: black line).